Yonezawa, Toshio; Hänninen, Hannu; Hashimoto, Atsushi

Weld Cracking Susceptibility of High-Cr Ni-Base Fe Alloys and Its Improvement—Development of Novel Test Method for Ductility-Dip Cracking and New Alloy

Published in:
Metallurgical and Materials Transactions A: Physical Metallurgy and Materials Science

DOI:
10.1007/s11661-024-07363-2

Published: 01/06/2024

Document Version
Peer-reviewed accepted author manuscript, also known as Final accepted manuscript or Post-print

Please cite the original version:
Yonezawa, T., Hänninen, H., & Hashimoto, A. (2024). Weld Cracking Susceptibility of High-Cr Ni-Base Fe Alloys and Its Improvement—Development of Novel Test Method for Ductility-Dip Cracking and New Alloy. *Metallurgical and Materials Transactions A: Physical Metallurgy and Materials Science* , *55*(6), 1878-1893. https://doi.org/10.1007/s11661-024-07363-2

Weld Cracking Susceptibility of High-Cr Ni-base Fe Alloys and Its Improvement

- Development of Novel Test Method for Ductility-dip Cracking and New Alloy

Toshio Yonezawa[1], Hannu Hänninen[2], Atsushi Hashimoto[3]
[1]Tohoku University (retired), Tagajyo, Higashi-Tanaka, 985-0863, Japan
[2]Aalto University, Espoo, Puumiehenkuja, 3, 02150, Finland
[3]Tohoku University, Sendai, Aoba, 980-8579, Japan

Corresponding Author: Toshio Yonezawa : toshio.yonezawa@gmail.com

ABSTRACT

The susceptibility to weld cracking such as Ductility-dip cracking (DDC), Liquation cracking and Solidification cracking, for laboratory melted high-Cr Ni-base Fe alloys was evaluated by Longi-Varestraint, strain to fracture (STF), on-heating on-cooling hot ductility, five-passes four-layer build-up (FPFLB) and axial tensile preloaded thermal cycling (TPLTC) tests, was compared with commercial Alloy 52. The on-heating on-cooling hot ductility and Longi-Varestraint tests showed similar cracking susceptibility, but they were not so suitable for the evaluation of DDC susceptibility. The DDC susceptibility for various materials was evaluated by the FPFLB, STF and TPLTC tests, and there are no significant inconsistencies for DDC susceptibility between the results of these tests. The TPLTC test which simulates the thermal history at the DDC detected location in FPFLB test specimen and the restrained stress in multi-pass welded joint was performed using the all weld metal round-notched bar specimens. Evaluation was performed by the number of thermal cycles until rupture. It was confirmed that the TPLTC test method is a novel test method that can be easily performed comparing with FPFLB and STF tests. A Nb and C containing 30%Cr Ni-base Fe alloy without Mo is suggested as an advantageous new DDC resistant weld metal.

Keywords: Ductility-dip cracking; High-Cr Ni-based alloy; Longi-Varestraint test; Five-pass four-layer build-up test; On-cooling hot ductility test; Tensile preloaded thermal cycling test; Thermal strain ratchetting

I. INTRODUCTION

It is well known that in case of austenitic steels and alloys, in addition to solidification cracking and liquation cracking, ductility-dip cracking (DDC) may occur as one type of the weld cracking. There is a consensus among researchers that the mechanism of solidification cracking is caused by the liquid film remaining at the dendrite boundaries during final solidification, and the mechanism of liquation cracking

is caused by the liquation of the eutectic substances at grain boundaries due to the heat effect of welding after solidification.[1]

However, regarding the mechanism of DDC, many hypotheses and evaluating test methods have been proposed so far, but there are still plenty of remaining unclear issues.

Therefore, in this study, the authors have reviewed first the proposed ductility-dip cracking mechanisms and their evaluation test methods in the past and recent activity related to new mechanisms and new evaluation test methods. Based on the review, the authors propose a new, unique and convenient evaluation test method for DDC and make a re-evaluation focusing on high-Cr Ni-based Alloy 52 variants with excellent DDC resistance.

In 1912 Bengough reported that Cu alloys, Al alloys, Cu-Ni alloys, etc. show a decrease in ductility in the medium to high temperature range, which is lower than the melting point. His paper summarized the past studies that reported similar results.[2] It was considered that the formation of an amorphous phase contributed to the phenomenon. Several discussions by other researchers on this paper were published, one of which was Hudson, who stated that the decrease in ductility in the medium to high temperature range is due to the decrease in ductility below the recrystallization temperature, and it has nothing to do with an amorphous phase.[3] Since then, many researchers have reported that austenitic stainless steels[4] and various alloys such as those of molybdenum, vanadium and titanium exhibit a decrease in ductility at medium to high temperatures.[e.g., [5-7]] In addition, Rhines et al. reported the decrease in ductility of Ni-Cr-Fe alloys at medium to high temperatures, where creep is a problem.[8] On these issues many studies have been conducted, and many test techniques for evaluating the solidification cracking, liquation cracking and ductility-dip cracking susceptibility of austenitic steels and alloys have been proposed. For example, longitudinal Varestraint test,[9, 10] trans-Varestraint test,[11] spot Varestraint test[12-14] or TIGAMAJIG,[15-17] mini Varestraint test,[18] secondary Varestraint test,[18] Heavy Welding Spot Varestraint test,[19] Moving Torch Varestraint test,[20] SIGMAJIG,[21-23] Circular Patch test,[24, 25] Hot Ductility test,[26] Cross Bead

Varestraint test,[27] Fissure Bend test,[28, 29] Strain to Fracture (STF) test,[30-34] Hot ductility tests during on-heating and on-cooling,[35,36] etc. have been developed. Along with the development of the test methods, much basic research on DDC has been made, as DDC occurs as an extremely troublesome phenomenon in the fabrication of large components.

Matsuda et al. investigated the effects of C, Si, Mn, P, S, O, N and Al contents on the DDC susceptibility of Invar alloy (Fe-36% Ni alloy), using the "Cross Bead Varestraint Test". They reported that high S, O, N and Al contents accelerate DDC, P content slightly accelerates it, and Si and Mn contents suppress it.[27] Furthermore, Nakao et al. performed "Cross Bead Varestraint Test" and "Hot Ductility Test" on 70Ni-0Cr-30Fe, 70Ni-10Cr-20Fe and 70Ni-20Cr-10Fe alloys at medium to high temperatures with varying amounts of P, Si and S.[37] They concluded that DDC of the 70Ni-Cr-Fe-0.007%S alloy occurs due to the decrease in ductility at 900~1000°C, which is caused by the grain boundary segregation of S. This tendency decreases with the increasing Cr content.

Since then many researchers have studied the mechanism of DDC from the microscopical point of view. The mechanism of DDC has been proposed to be grain boundary sliding and void formation at the grain boundaries. Collins, Lippold[38], Collins, Ramirez, Lippold[39] and Ramirez, Lippold[40, 41] reported that the grain boundary orientation to the applied strain and triple-point grain boundary intersections are the contributing factors to DDC formation and initiation.[38] They concluded that the DDC is an elevated temperature grain boundary sliding mechanism, and such sliding can be opposed macroscopically by the formation of tortuous grain boundaries via a grain boundary pinning mechanism.[39] They proposed also highly DDC-resistant materials.[42]

Furthermore, Noecker and DuPont reported that DDC in the Ni-base Cr-Fe alloys appears to be caused by grain boundaries that may be exacerbated by highly localized stresses, and these stresses may develop along the matrix/precipitate interfaces when $M_{23}C_6$ carbides form in the same time/temperature regime as

the hot ductility test.[35,36] Recently, McCracken et al. proposed the new mechanism for DDC. They reported that a new high-restraint narrow groove test mock-up was successfully developed to confirm the proposed thermal strain ratchetting effect on DDC susceptibility, and the thermal strain ratchetting has a greater effect on DDC occurrence than the actual magnitude of cumulative plastic strain.[43,44] Still, there are many unknown issues related to the DDC occurrence.

In this study the authors try to evaluate the effects of the chemical composition (especially C, Si, Mn, Fe, Al, Nb and Ti contents) of the high-Cr Ni-base Alloy 52 variants on the susceptibility to weld cracking such as Solidification cracking, Liquation cracking and DDC, and the Longi-Varestraint test was performed for all the laboratory melt heats first. According to the results of the Longi-Varestraint tests, the authors compare the weld cracking susceptibility of various high-Cr Ni-base Alloy 52 variants using various test methods that have been reported by other researchers to evaluate DDC susceptibility.

Moreover, based on the recent thermal strain ratchetting mechanism hypothesis, the authors performed the thermal strain ratchetting tests using all-deposited weld metal specimens from the point of view of the mechanics of materials. That is, the thermal strain ratchetting phenomenon is a phenomenon that occurs when the material strength properties deteriorate due to repeated three-dimensional local plastic strain[45, 46, 47].

Therefore, in this study, the authors considered that the thermal strain ratchetting susceptibility can be evaluated more easily and quantitatively by employing round bar tensile test specimens made of all-deposited weld metal with a round notch and applying cyclic thermal stress and strain. The Tensile Pre-Loaded Thermal Cycling (TPLTC) tests were conducted, to compare the~~ir~~ thermal strain ratchetting resistance of the studied weld metals with the DDC susceptibility results obtained by various DDC evaluation test methods used in the literature[48,49].

Based on the results, whether or not the DDC is caused by the thermal strain ratchetting, and the performance of the new thermal strain ratchetting evaluation test method, the authors propose a new DDC-resistant high-Cr Ni-base Alloy 52 variant.

II. EXPERIMENTAL PROCEDURES

A. *Test Material*

In order to compare the weld cracking susceptibility by Longi-Varestraint test with the DDC susceptibility using reported DDC test techniques and the new thermal strain ratchetting evaluation test method of various high-Cr Ni-base Alloy 52 variants and commercial Alloy 52 a large number of various alloys was manufactured. As the high-Cr Ni-base Alloy 52 variants, the laboratory melt Heats No.1 to No.10, 09R/TD9, 69B, VT, WT, B1 and B2 were used. As the reference materials, commercial filler wire of Alloy 52 and simulated Alloy 52MSS (Sim.52MSS), which has the simulated chemical composition of Alloy 52MSS, but is not a commercial Alloy 52MSS,[50] were used. Heats No.1, 2, 4 to 9, VT, WT, XT, ZT, B1 and B2 are 30%Cr Ni-base~~d~~ Fe alloys with controlled C, Si, Mn, Nb, Ti and Al contents. Heat No. 3 and No.10 have simulated chemical compositions of Alloy 52 and 132, respectively. Heat 69B has the simulated chemical composition of Alloy 690. The chemical compositions of the ~~17~~19 laboratory melt heats and commercial Alloy 52 are shown in Table 1.

Table 1 Chemical compositions of all test materials (wt%, check analysis for button melts, ladle analysis for others).

No.	Features		Chemical compositions (wt%, check analysis for button melt, ladle analysis for others)											
			C	Si	Mn	P	S	Ni	Cr	Fe	Mo	Al	Nb	Ti
No.1	1kg button lab. melt	Modified Alloy 52, high Si, Mn	0.019	0.72	2.18	0.005	0.0008	56.30	29.96	9.04	-	0.816	0.08	0.81
No.2		Modified Alloy 52, low Si, Mn	0.028	0.10	0.10	0.005	0.0017	58.94	30.04	9.04	-	0.815	0.09	0.80
No.3		Simulated Alloy 52	0.024	0.35	0.99	0.005	0.0010	57.88	29.94	9.02	-	0.816	0.08	0.80
No.4		30%Cr-Ni base 7%Fe, high Mn	0.023	0.36	2.17	0.005	0.0010	58.50	30.10	7.06	-	0.794	0.08	0.80
No.5		30%Cr-Ni base 5%Fe, high Mn	0.022	0.37	2.18	0.005	0.0010	60.72	29.90	5.02	-	0.787	0.08	0.81
No.6		30%Cr-Ni base 3%Fe, high Mn	0.023	0.35	2.18	0.005	0.0009	62.53	30.08	3.04	-	0.786	0.08	0.80
No.7		30%Cr-Ni base 1.5%Fe, high Mn	0.023	0.36	2.19	0.005	0.0008	63.99	30.09	1.56	-	0.787	0.08	0.80
No.8		30%Cr-Ni base 0.5%Fe, high Mn	0.022	0.37	2.17	0.004	0.0009	65.70	29.96	0.43	-	0.795	0.08	0.80
No.9		Pure 30%Cr-Ni base 3%Fe, low C, Si, Al, Nb, Ti	0.006	0.10	0.99	0.005	0.0005	65.80	29.94	3.05	-	<0.002	<0.002	0.002
N0.10		Modified Alloy 132, high Mn, med. Nb, low C, Al, Ti	0.007	0.22	2.8	0.003	0.0008	70.50	14.98	9.48	-	<0.003	1.81	<0.002
B1		30%Cr-Ni base 7%Fe, high C, Nb, low Si, Al	0.030	0.01	0.96	≦0.001	0.0010	55.85	30.19	6.90	≦0.01	0.19	2.47	0.30
B2		30%Cr-Ni base 7.5%Fe, med. C, Nb, low Si, Al	0.023	0.01	0.98	≦0.001	≦0.001	58.70	30.08	7.55	≦0.01	0.19	1.97	0.30
Sim.52MSS		Simulated Alloy 52MSS	0.020	0.01	0.97	≦0.001	0.0010	58.71	30.15	3.00	4.02	0.19	2.47	0.30
09R/TD9	50kg VIM lab. melt	30%Cr-Ni base 2.6%Fe, low C, Si, Al, Nb, Ti	0.005	0.12	0.53	≦0.002	0.0006	66.22	30.38	2.60	-	0.064	≦0.002	0.003
VT		30%Cr-Ni base 9%Fe, med. C, low Si, Al, Nb, Ti	0.016	0.10	0.52	≦0.001	0.0010	59.96	30.1	8.92	-	0.046	0.10	0.25
WT		30%Cr-Ni base 9%Fe, med. C, Nb, Ti, low Si, Al	0.020	0.13	0.51	≦0.001	0.0010	60.10	29.86	8.92	-	0.086	0.069	0.35
XT		30%Cr-Ni base 9%Fe, med. C, high Nb, low Si, Al	0.021	0.12	0.53	0.001	≦0.001	60.47	28.02	8.10	-	≦0.005	2.62	0.33
ZT		30%Cr-Ni base 9%Fe, low C, Si, Al, Nb, Ti	0.003	0.10	0.5	0.004	≦0.001	60.09	29.89	9.54	-	0.036	≦0.01	≦0.001
69B		Simulated Alloy 690, high C, low Nb	0.032	0.18	0.31	0.006	0.0010	59.8	30.2	8.61	-	0.35	≦0.002	0.35
Alloy 52	Filler wire	Commercial Alloy 52	0.027	0.16	0.24	0.002	≦0.001	60.52	28.8	8.99	0.01	0.71	0.01	0.50
AWS A5.14 ER NiCrFe-7 (UNS N06052) specification			≦0.04	≦0.50	≦1.0	-	≦0.015	Bal.	28.0-31.5	7.0-11.0	-	≦1.10	≦0.10	≦1.0

: Reduced element compared from Alloy 52

: Increased element compared from Alloy 52

The laboratory melt Heats No. 1 to No. 10, B1, B2 and Sim.52MSS were melted by 1 kg button melting process in vacuum, fabricated to the strips of 5.5 mm thick, 50 mm long and 70 mm wide, machined into square bars with a cross-section of 5.5 mm and welded together to form a 1.6 mm diameter wire using the cold pilger wire reducing process.

The laboratory melted Heats 09R/TD9, 69B, VT and WT were manufactured by 50 kg vacuum induction melting (VIM) process and the ingots were soaking heat treated at 1200 °C. Halves of these 50 kg VIM ingots were hot forged to the bars of 70 mm diameter. These bars were fabricated to the 1.6 mm diameter filler wires by hot rolling and cold pilger wire reducing process.

Other halves of Heat 69B, VT and WT VIM ingots were hot forged and hot rolled to 20 mm thick and 70 mm wide sheets. These sheets were solution heat treated at 1100 °C for 1 hour. Some of the 20 mm thick and 70 mm wide sheets were fabricated to the strips of 5.5 mm thick, 50 mm long and 70 mm wide.

The commercial Alloy 52 filler wire of 1.6 mm diameter was obtained from Special Metals Co.

B. *Weld Cracking Susceptibility by Various Tests*

B.1 *Longi-Varestraint Test*

Weld cracking susceptibility is categorized as Solidification Cracking, Liquation Cracking, and Ductility-Dip Cracking as explained in Introduction and for convenience, these phenomena are often referred to as hot cracking. Although many types of Varestraint tests have been developed, the Longi-Varestraint test is commonly used as a Varestraint test that can comprehensively evaluate the hot cracking susceptibility[9, 10]. Therefore, in this study, we evaluated first the hot cracking susceptibility of high-Cr Ni-base alloys using the Longi-Varestraint test.

In this study, two 10 mm thick, 70 mm wide and 150 mm long carbon steel support strips were added to each 5.5 mm thick, 50 mm wide and 70 mm long samples of the 17 laboratory melt heats by TIG welding, as shown in Fig. 1. Using these welded strips as the test specimens, the Longi-Varestraint tests were conducted under the conditions of 125A of welding current, 10 V of welding voltage, 8

cm/min of welding travel speed and augmented strain was selected between about 1 to 13%. After the Longi-Varestraint tests, the number of cracks, total length and maximum length of cracks were measured by a stereo microscope.

Fig. 1 Longi-Varestraint test specimen with carbon steel support strips welded to each end.

B.2 *On-heating On-Cooling Hot Ductility Test*

On-heating on-cooling hot ductility test reported by Noecker and DuPont,[35,36] was performed using wires of the laboratory melted Heat 09R/TD9, Heat 69B and commercial Alloy 52. The large two-pass beads were deposited on the laboratory melted Heat 69B plates, which were machined from 20 mm thick and 70 mm wide sheets, under the conditions of 200 A of welding current, 12.5 V of welding voltage, 10 cm/min of welding travel speed, 170 cm/min of wire feed rate and less than 100 ºC of interpass temperature of each bead, using the laboratory melted Heat 09R/TD9 and commercial Alloy 52 filler wires.

The on-heating on-cooling hot ductility test specimens were machined from the large two-pass beads and the heat-affected zone (HAZ) of the base plates by the large two-pass beads built. The appearance of the typical large two-pass beads is shown in Fig. 2 a) and the configuration of the on-heating on-cooling hot ductility test specimen is shown in Fig. 2 b).

The on-heating hot ductility test was performed at 51 ºC intervals between 800 ºC and 1,000 ºC at the heating rate of 111 ºC/s. The on-cooling hot ductility test was performed at 51 ºC intervals at the cooling rate of 50 ºC/s after heating up to 1100 ºC. 99.995% Ar gas was used to augment the cooling rate of the “on-cooling” specimens.

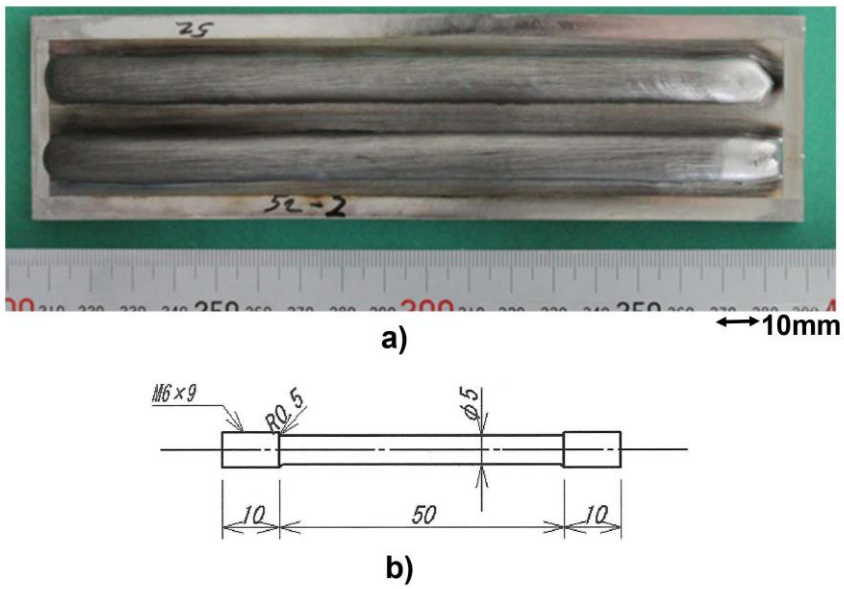

Fig. 2 The appearance of the typical large two-pass beads on the base plate of laboratory melted Heat 69B (a), the configuration of the on-heating on-cooling hot ductility test specimen machined from the center of the large two-pass beads, and heat-affected zone of the base plate (b).

B.3 *Strain to Fracture Test*

The Strain to Fracture (STF) test specimens of the laboratory melted Heat 09R/TD9 and commercial Alloy 52 were manufactured as follows:

1) Prior to machining specimens from the plate material of carbon steel~~.~~, continuous automatic gas tungsten arc welds (GTAW) using the laboratory melted Heat 09R/TD9 and commercial Alloy 52 wires were made at the reduced section on one side of the carbon steel plate at the locations coinciding with the test section of the STF specimens with a nominal width of 15 mm, as shown in Fig. 3a) (The STF specimens were machined along the dashed lines). The continuous automatic GTAW on the carbon steel plate was conducted under condition of 250 A of welding current, 11.5 V of welding voltage, 10 cm/min of welding travel speed, 175 cm/min of wire feed rate, less than 100 ºC of interpass temperature and 20 ℓ/min of gas flow.

After machining specimens from the GTA welded plate material of carbon steel, ~~A~~an autogenous GTA spot weld was then performed within the reduced section of the machined specimen on the

opposite side of the continuous GTA weld. The diameter of the spot weld was nominally 10mm, approximately two-thirds of the width of the reduced section, as shown in Fig. 3b).

2) The specimen was placed in a copper fixture to prevent reheating of the continuous weld. Using these specimens, the STF tests were performed at 800 to 1150 °C under 1 to 18.5% applied strain.

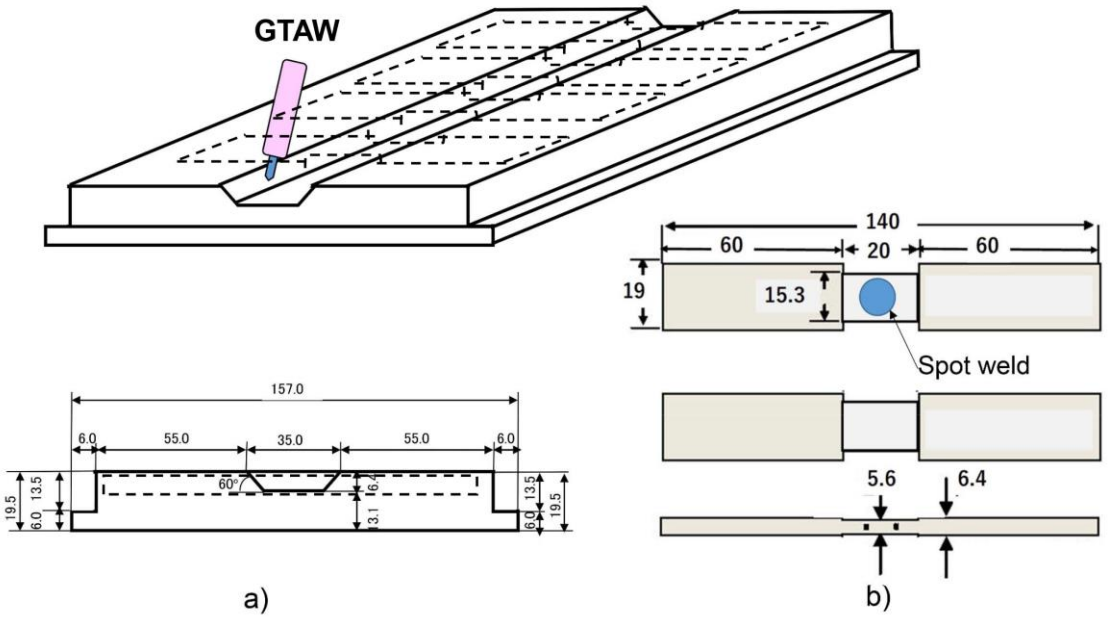

Fig. 3 Preparation and configuration of STF specimen. (a) The cross-section and bird's eye view of GTA welding at the reduced section on one side of the carbon steel plate, along the centerline of machined specimens. The weld metal was deposited with GTA welding (GTAW) on one side of the carbon steel plate by commercial Alloy 52 and laboratory melted 09R/TD-9 wires. After GTAW, the STF samples were machined along dashed lines. (b) After the STF specimens were machined from welded carbon steel plate, the STF specimens were spot welded by autogenous GTAW on one side at the center of the STF specimens.

B.4 *Five-Pass Four-Layer Build-up Test*

The Five-Pass Four-Layer Build-up (FPFLB) test specimens were fabricated by the five-pass for one layer and four-layer build-up on the laboratory melted Alloy 690 (69B in Table 1) test coupon and

finally the five-pass of wash beads were done on the top of the FPFLB specimen, as shown in Fig. 4. (The DDC of high-Cr Ni-base Alloy 52 variants is usually observed in multi-layered weld metal.)

The FPFLB test specimen is very similar to the Narrow groove welds by McCracken.[41,43,45] The FPFLB test specimen is 22 cm long and 3 cm wide. The FPFLB test specimen was welded under conditions of 100 A of welding current, 10.5 V of welding voltage, 12 cm/min of welding travel speed, 28 cm/min of wire feed rate and less than 100 °C of interpass temperature. Each FPFLB test specimen was cut to 5 pieces perpendicular to the beads. The type and the number of cracks of each type were evaluated on the 4 cross-sections of FPFLB test specimens by an optical microscope.

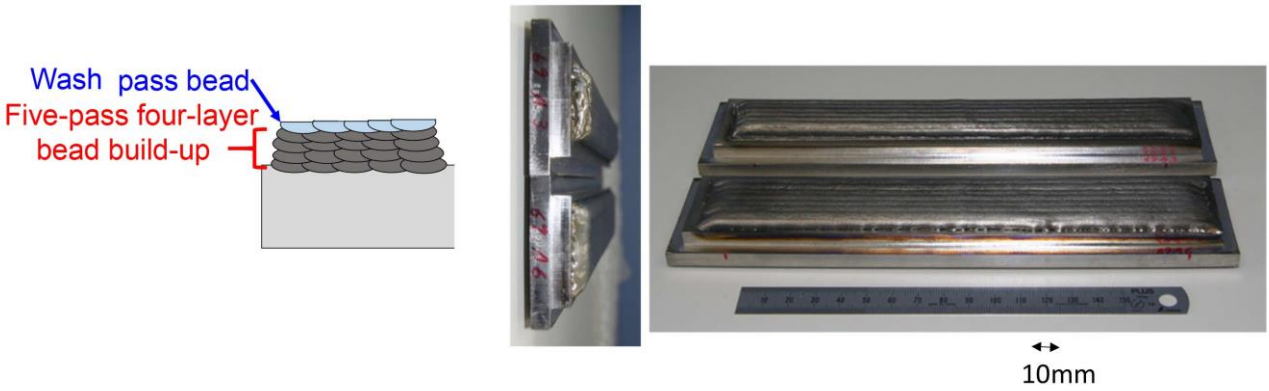

Fig. 4 Configuration of the FPFLB build-up specimen.

B.5 *Tensile Preloaded Thermal Cycling Test*

In order to confirm the DDC thermal strain ratchetting mechanism and to develop the new DDC test method based on the mechanics of materials and to develop the new DDC-resistant alloy, the axial tensile preloaded thermal cycling (TPLTC) test was performed. The TPLTC test specimen is machined from the large two-pass beads build-up by the test weld materials on the laboratory melt Alloy 690 (69B) plate material (as shown in Fig. 2 a)), and this specimen is a tensile test type bar specimen with a round notch, as shown in Fig. 5 a). The TPLTC test simulates the thermal cycling history in the FPFLB test specimen and the restraining stress of the multi-pass weld joint. In this study, in order to estimate the thermal cycling history near the estimated most sensitive DDC region

(the DDC was estimated to initiate first along the weld pass boundaries in the 2nd pass layer) of the FPFLB test specimen, the surface temperature of the bead of 1st pass in the 2nd pass layer was measured by an optical pyrometer as well as after 2nd pass in the 2nd pass layer to the final wash pass. The restraining stress applied to the multi-pass welded joint normally greatly exceeds the yield stress and is near the tensile strength of weld metal. Thus, the novel TPLTC test was conducted by the thermal cycling under 46 MPa tensile preload, which is the lowest measured tensile strength of the weld metals at elevated temperature, using a Gleeble test machine and the vacuum chamber. A thermal strain ratchetting usually occurs, when a multi-dimensional thermal cycle as a secondary stress acts under tensile preload or hoop-stress due to inner pressure as the primary stress. So, when an axial tensile preload and thermal cycling are applied to the TPLTC specimen, the tri-axial stress is repeated under the axial tensile preload in the vicinity of the round notched region, and thermal strain ratchetting will occur. The tensile preload value of 46 MPa was selected based on the minimum tensile strength of all the test materials at 1200 ^{o}C, 36 MPa, multiplied by the stress concentration factor of 1.42 and using a margin of 90%.

Heating up was conducted by a high-frequency induction heating device to obtain a uniform heating of the notch region, and cooling down was made by high purity Ar gas (99.995 % spec. grade) injection. The first heating up was conducted in vacuum environment and after the first cooling down all heating and cooling cycles were conducted in high purity Ar gas environment, to continue thermal cycling testing without any interruption. Before the novel TPLTC test, a Platinum Platinum-Rhodium (Pt Pt-Rh) thermocouple was attached to the surface of the round notch location of the test specimen as shown in Fig. 5 b).

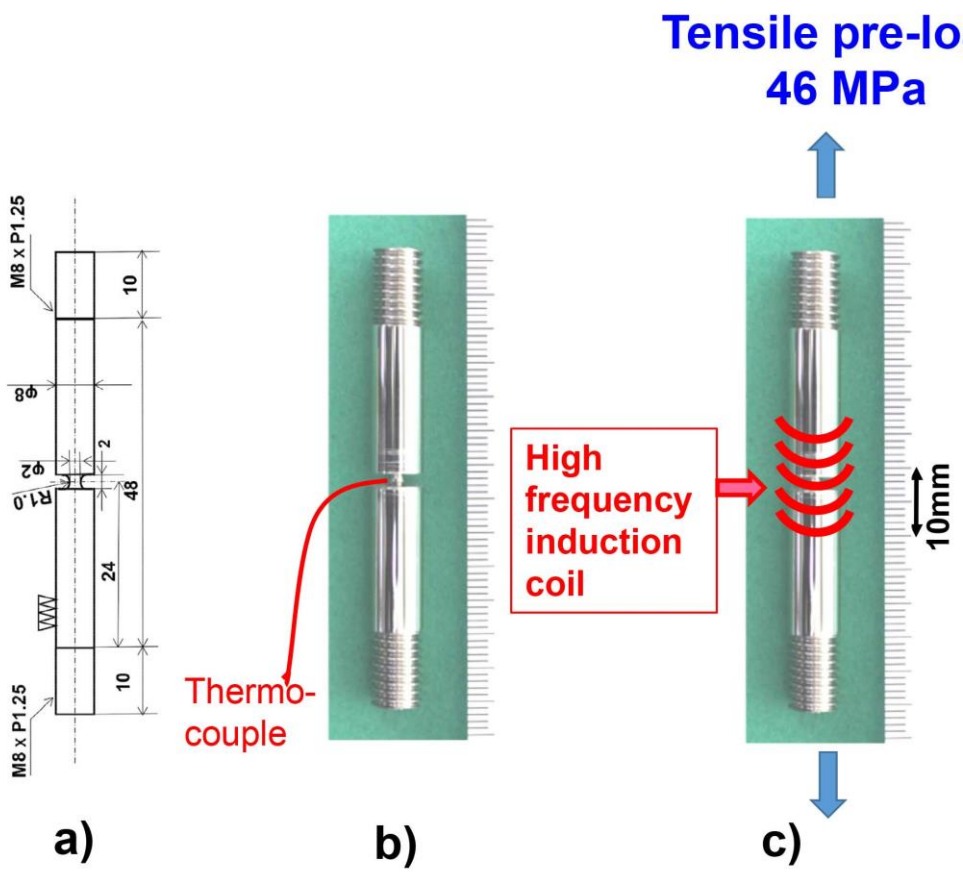

Fig. 5 The TPLTC test using round-notched tensile test specimen (dimension is as shown in Fig. 5 a)) made of all-deposited weld metal. The temperature cycles of the TPTLC specimen were continuously measured using a Pt Pt-Rh thermocouple attached to the surface of the round notch of the TPTCL specimen, as shown in Fig. 5b). The thermal cycling was performed to the TPLTC test specimen according to Table 2. Axial tensile preloading was 46MPa, heating up was applied by a high-frequency induction coil (as shown in Fig. 5c)), and cooling down was conducted by high purity Ar gas.

The heating/cooling cycles from (1) to (10) simulate the thermal cycling history at the estimated DDC location of the FPFLB test specimen during five-pass four-layer build-up welding. The lowest temperature of the thermal cycles is the controlled interpass temperature for the FPFLB test specimen. The peak temperature after 11 cycles in the FPFLB test specimen is a little lower than that in the (1) to (10) cycles, but in order to accelerate the effect of thermal cycling the

heating/cooling cycles are repeated as from (1) to (10). The thermal cycling was performed under the axial tensile preload of 46 MPa until rupture of the specimen, and the number of heating/cooling cycles at the time of rupture was determined. Also, the crack initiation temperature and rupture temperature of the test specimen are obtained from the temperature recording chart. The heating/cooling cycles from (1) to (10) are shown in Table 2.

Table 2 Test conditions of Tensile Preloaded Thermal Cycling test (Tensile preload is 46MPa).

No. of Cycle	Starting T (ºC)	Heat-up Target T (ºC)	Heat-up Time & Atmosphere	Cooling Target T (ºC)	Cooling Rate & Atmosphere
1	Room T	1200	10 sec. in Vacuum	200	50ºC/sec in Ar gas
2	200	1100	10 sec. in Ar gas	200	50ºC/sec in Ar gas
3	200	1000	10 sec. in Ar gas	200	50ºC/sec in Ar gas
4	200	900	10 sec. in Ar gas	200	50ºC/sec in Ar gas
5	200	800	10 sec. in Ar gas	200	50ºC/sec in Ar gas
6	200	700	10 sec. in Ar gas	200	50ºC/sec in Ar gas
7	200	800	10 sec. in Ar gas	200	50ºC/sec in Ar gas
8	200	900	10 sec. in Ar gas	200	50ºC/sec in Ar gas
9	200	1000	10 sec. in Ar gas	200	50ºC/sec in Ar gas
10	200	1100	10 sec. in Ar gas	200	50ºC/sec in Ar gas

Note: If the test specimen did not rupture in up to 10 thermal cycles, test was repeated from cycle 1 as cycle 11, and if the specimen did not rupture in up to 20 cycles, test was repeated from cycle 1 as cycle 21. The thermal cycling was continued until specimen rupture. The starting temperature for cycle 1 was room temperature, but for cycles 11, 21, or 31, etc., the starting temperature was 200°C. The atmosphere in cycle 1 was vacuum, but in cycles 11, 21, or 31, etc., it was high purity Ar gas.

III. RESULTS AND DISCUSSIONS

A. *Weld Cracking Susceptibility by Various Tests*

In this study, the weld cracking susceptibility of high-Cr Ni-base Alloy 52 variants using various test methods, focusing on DDC susceptibility, was examined and the following results were obtained.

A.1 *Longi-Varestraint Test*

The typical magnified outer appearance of the Longi-Varestraint test specimens near the maximum augmented strain region after the test is shown in Fig. 6.

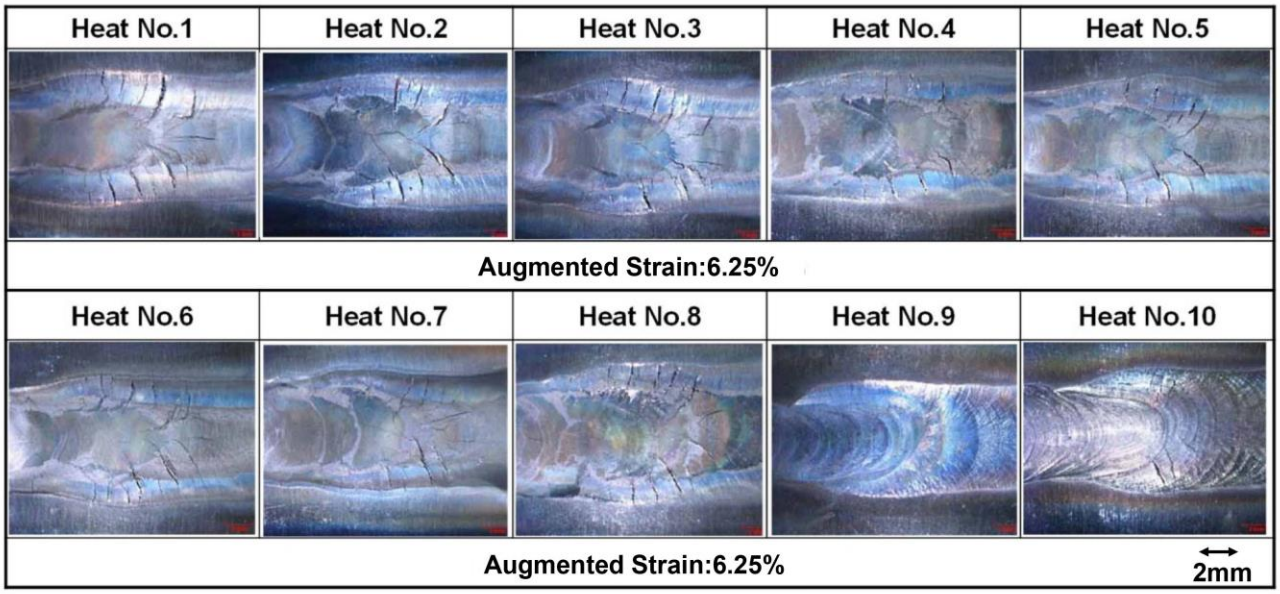

Fig. 6 Examples of magnified outer appearance of the Longi-Varestraint test specimens near the maximum augmented strain region after the test.

All test results of the Longi-Varestraint test for the 17 laboratory melt heats are summarized in Fig. 7. Figure 7 a) shows the number of detected cracks versus augmented strain and Fig. 7 b) shows the total length of detected cracks after Longi-Varestraint test. The Longi-Varestraint test data for Heats No. 1 to No. 10 are connected by fine dashed lines and the data for the other heats are connected by broad straight lines.

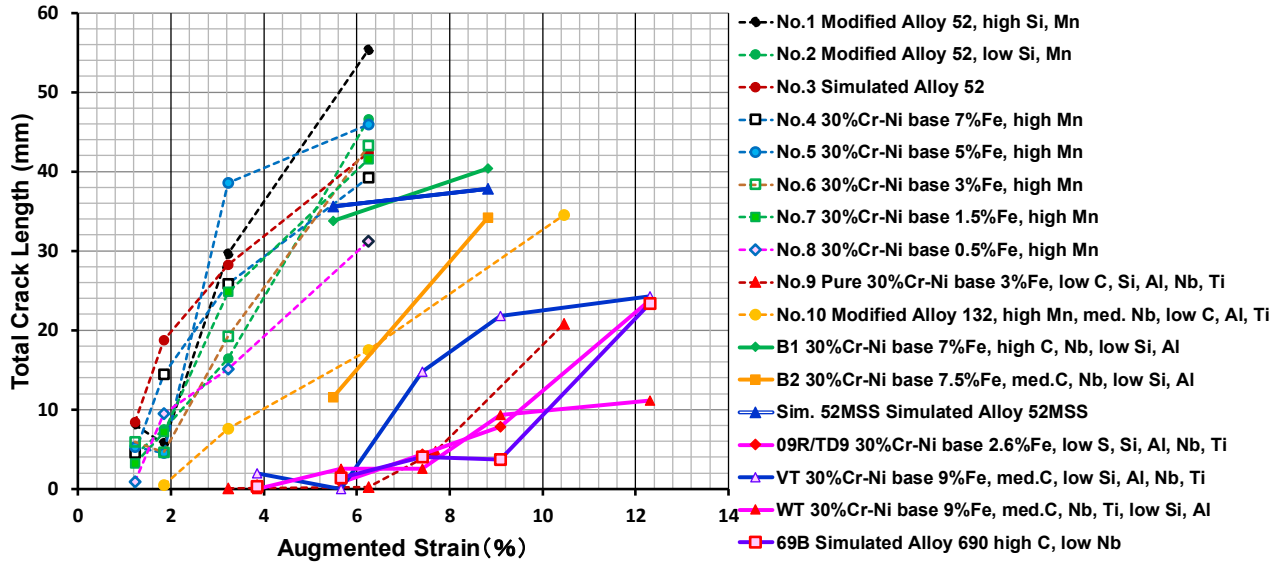

a)

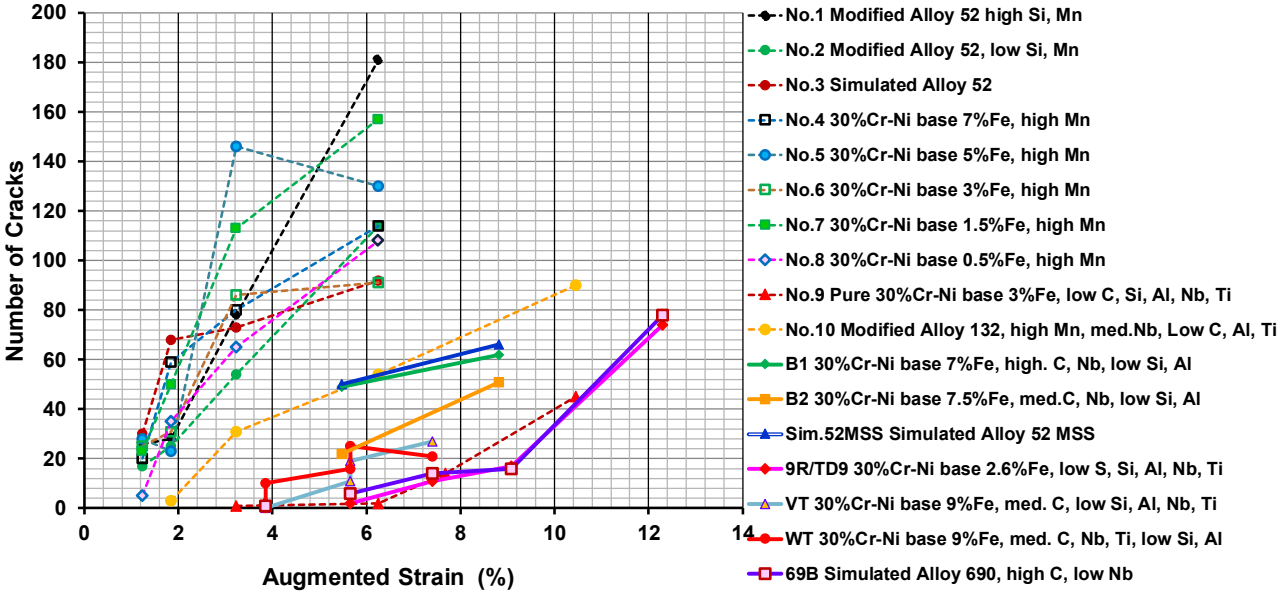

b)

Fig. 7 Hot cracking susceptibility of all test materials by Longi-Varestraint test. (a) Number of cracks vs. augmented strain (%) and (b) Total crack length vs. augmented strain (%).

Heats 09R/TD9, VT, WT, XT and ZT show better cracking resistance by the Longi-Varestraint test comparing with the laboratory melt Heat No. 3 (simulated Alloy 52) and Heat No. 10 (simulated

Alloy 132). Heat B1 showed similar cracking resistance to Heat No. 10, but was better than Heat B2 and Heat Sim.52MSS by the Longi-Varestraint test.

~~B.~~ A.2 *On-heating On-Cooling Hot Ductility Test*

In order to confirm the presence of ductility reduction in the medium to high temperature range, the "on-heating on-cooling hot ductility test" which simulated the reports by Noecker and DuPont [35.36] was performed using the specimens machined from all-deposited weld metal and HAZ of the base metal. The hot ductility loss by on-cooling is more sensitive than that by on-heating for Heat 69B, which is simulated Alloy 690, as shown in Fig. 8. This result confirms the same behavior as reported by Noecker and DuPont[35,36]. The all-deposited weld metal specimens of commercial Alloy 52 filler wire showed a ductility loss at 900 to 1000º C, but the all-deposited weld metal specimens of laboratory Heat 09R/TD9 wire (similar chemical composition as Heat No. 9) and HAZ of the Heat 09R and 69B base plate showed no remarkable ductility loss at 800 to 1000 º C, as shown in Fig. 9.

There seems to be no significant differences between the high cracking susceptibility of Sim. Alloy 52 by the Longi-Varestraint test and the ductility decrease by the on-cooling hot ductility test for the commercial Alloy 52. Thus, the on-heating on-cooling hot ductility test may not correctly evaluate the DDC susceptibility. These test results in this study are different from the research results by Noecker and DuPont.[35,36]

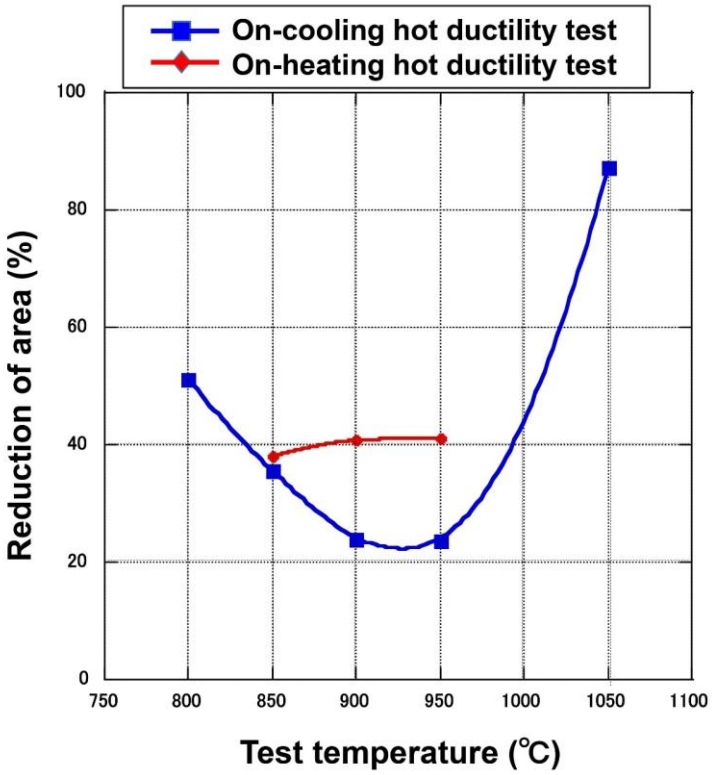

Fig. 8 On-heating on-cooling hot ductility test results for laboratory melted Heat 69B.

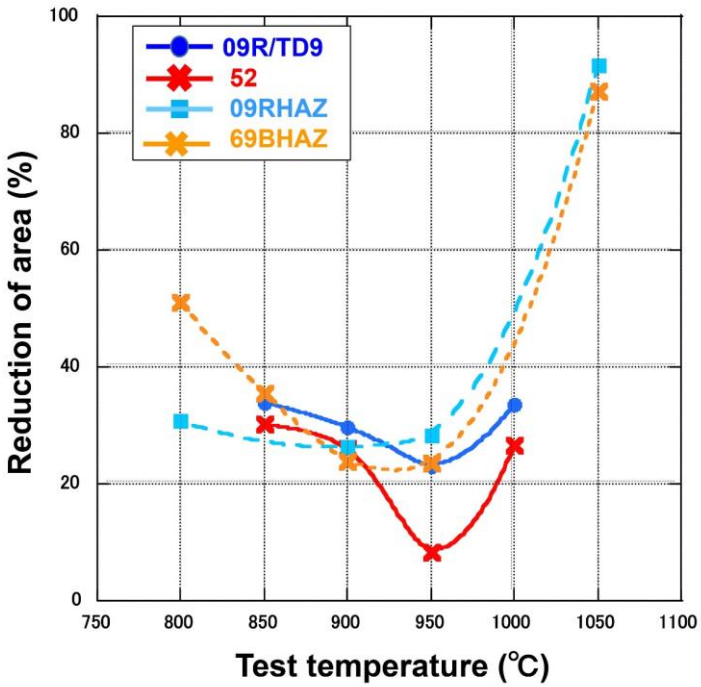

Fig. 9 On-cooling hot ductility test results for laboratory melted Heats 09R/TD9 and 69B and commercial Alloy 52.

A3. *Strain to Fracture Test*

The Strain to Fracture (STF) test results of commercial Alloy 52 and laboratory melt Heat 09R/TD9 are summarized in Fig. 10. The laboratory melt Heat 09R/TD9 is more susceptible to DDC than the commercial Alloy 52. The temperature range at which cracking susceptibility is most remarkable is 900°C to 1000°C, which is not significantly different from the results of Nissley and Lippold[42,51]. However, regarding the mechanism of DDC the role of thermal cycling has been put forward due to the thermal strain ratchetting phenomenon.[43,44] The test methods evaluating only the fracture strain in the temperature range of reduced ductility without applying thermal cycling, such as the STF test, may not be sufficient for evaluating the DDC susceptibility.

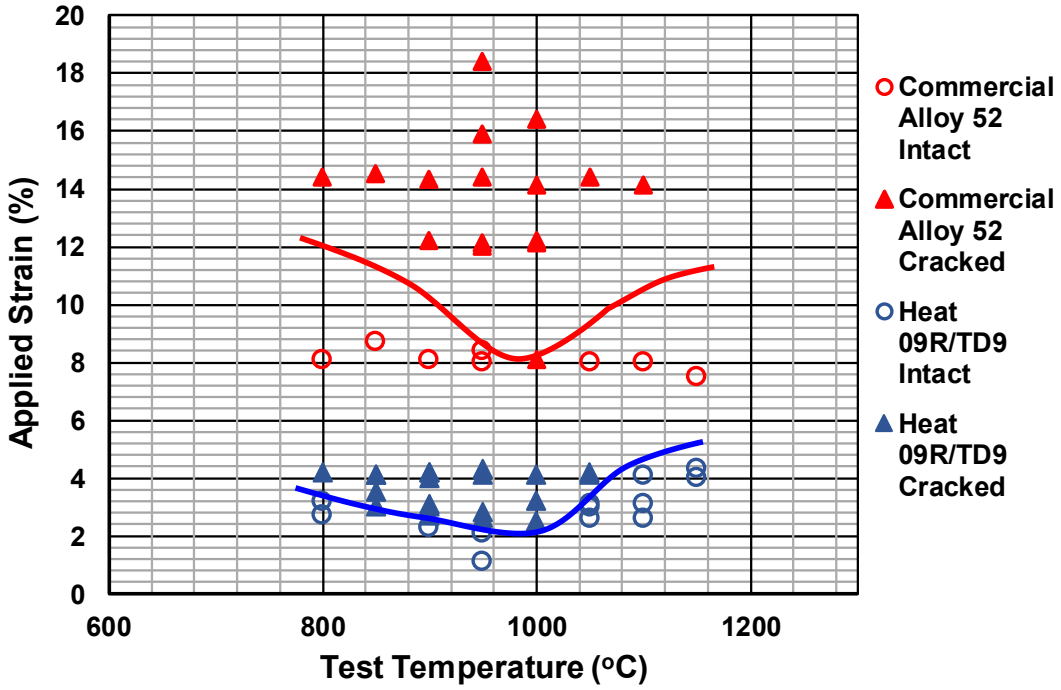

Fig. 10 STF test results for commercial Alloy 52 and laboratory melted Heat 09R/TD9.

A4. *Five-Pass Four-Layer Build-up Test*

The Five-Pass Four-Layer Build-up (FPFLB) test specimens were made by depositing four layers of five beads each on the laboratory melt Alloy 690 plate (69B) with a final wash bead treatment on the final layer following wash bead treating technique on the laboratory melt Alloy 690 plate, using the commercial Alloy 52 and laboratory melted Heat 09R/TD9 wires, as shown in Fig. 11.

The specimens were cross-sectioned and observed by optical microscopy after polishing and etching by aqua regia. No cracks were observed in any cross-section of the specimens made by commercial Alloy 52 wire, but many cracks were detected in the specimens made by laboratory melted Heat 09R/TD9 wire, as shown in Fig. 11. The evaluation of cracking susceptibility by the Longi-Varestraint test and on-cooling hot ductility test is quite different from that observed by the FPFLB test.

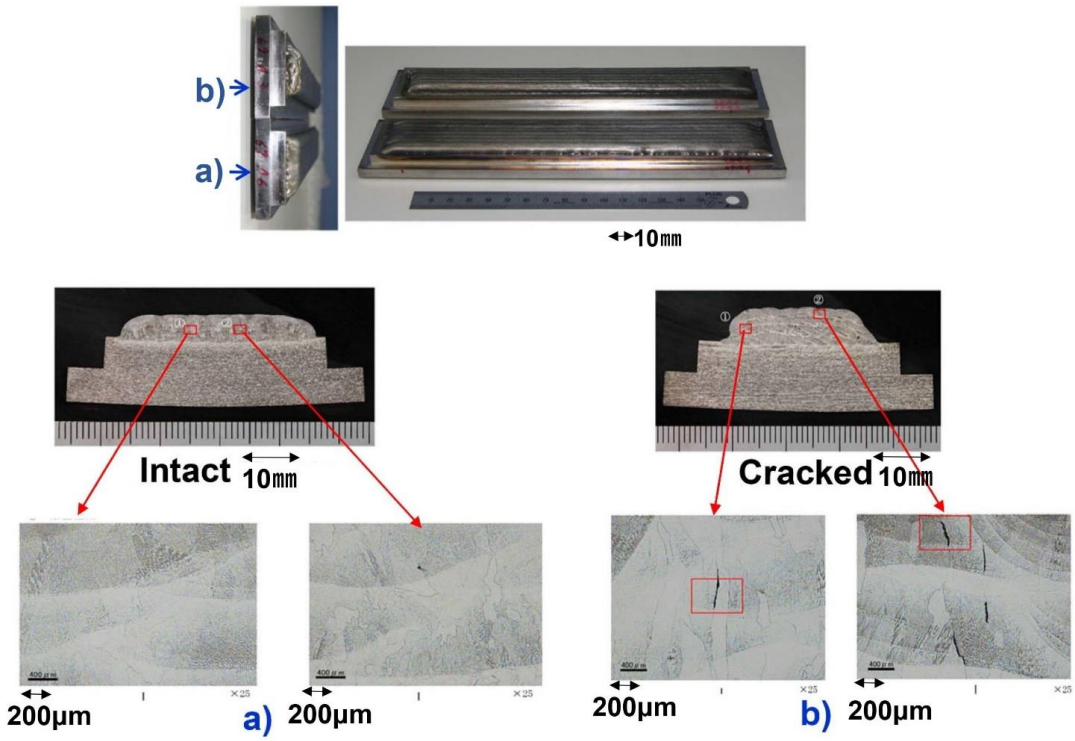

Fig. 11 Appearance and microscopy of the cross-sections of FPFLB build-up and wash bead test specimens using commercial Alloy 52 (a) and laboratory melted Heat 09R/TD9 wires (b).

The FPFLB test results for the 7 heats, which are commercial Alloy 52, Heats VT, WT, 09R/TD9, B1, B2 and Sim.52MSS, are summarized in Fig. 12. The DDCs observed on the cross-sections of FPFLB test specimens were categorized to Type I (connected voids), Type II (tight crack) and Type III (open crack), and the total number of categorized Type II and Type III cracks was compared in all the heats. The total number of categorized Type II and Type III cracks was the highest in Heat VT,

and decreased in the order of Heats WT, 09R/TD9 and 52, and was zero for Heats B1, B2 and Sim.52MSS. Thus, Heats B1, B2 and Sim.52MSS showed the highest resistance to DDC according to the FPFLB test results. The weld metal with a high DDC susceptibility (09R/TD9) in the FPFLB test did not show a decrease in ductility in the medium to high temperature range.

As shown in Fig.13, the observed cracks located at dendrite boundary or grain boundary under wash pass in the 4th bead layer were mostly Type I, the cracks located at dendrite boundary or grain boundary in the 3rd bead layer were Type I and Type II, and the cracks located at dendrite boundary or grain boundary in the 2nd bead layer were mostly Type II and Type III. It is considered that the DDCs grow from Type I crack to Type II crack and Type III crack according to the increasing thermal cyclic stress and strain. The authors estimated that the first DDC initiation region is located in 1st pass of the 2nd bead layer.

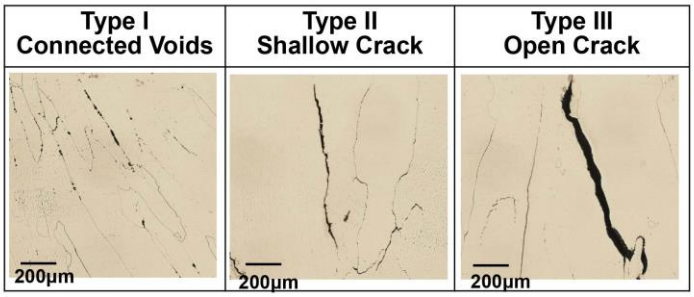

52 : 0.027C-29Cr- 9Fe-0.7 Al- 0.01 Nb-0.5 Ti
VT : 0.016C-30Cr- 9Fe-0.05Al- 0.1 Nb-0.25Ti
WT : 0.020C-30Cr- 9Fe-0.09Al- 0.07Nb-0.35Ti
09R/TD9:0.005C-30Cr-2.6Fe-0.06Al-0.002Nb-0.003Ti
B1 : 0.030C-30Cr-6.9Fe-0.19Al-2.47 Nb-0.30Ti
B2 : 0.023C-30Cr-8.0Fe-0.19Al-1.97 Nb-0.30Ti
52MSS : 0.020C-30Cr-3.0Fe-0.19Al-2.47 Nb-0.30Ti-4.0Mo

Heat	Ⅰ	Ⅱ	Ⅲ	Σ	Heat	Ⅰ	Ⅱ	Ⅲ	Σ	Heat	Ⅰ	Ⅱ	Ⅲ	Σ	Heat	Ⅰ	Ⅱ	Ⅲ	Σ
52	3	0	0	0	VT	>50	27	21	48	B1	0	0	0	0	52 MSS	0	0	0	0
	1	0	0	0		>50	10	11	21		0	0	0	0		0	0	0	0
	0	0	1	1		>50	24	25	49		0	0	0	0		0	0	0	0
	12	0	1	1		>50	30	18	48		0	0	0	0		0	0	0	0
Heat	Ⅰ	Ⅱ	Ⅲ	Σ	Heat	Ⅰ	Ⅱ	Ⅲ	Σ	Heat	Ⅰ	Ⅱ	Ⅲ	Σ					
WT	21	4	25	21	09R/ TD9	>50	1	0	1	B2	0	0	0	0	Σ = Ⅱ + Ⅲ				
	18	3	21	18		>50	3	0	3		0	0	0	0					
	25	3	28	25		>50	12	0	12		0	0	0	0					
	28	10	38	28		>50	1	0	1		0	0	0	0					

Fig. 12 Summary of detected micro-cracks on the cross-sections of FPFLB tested alloys.

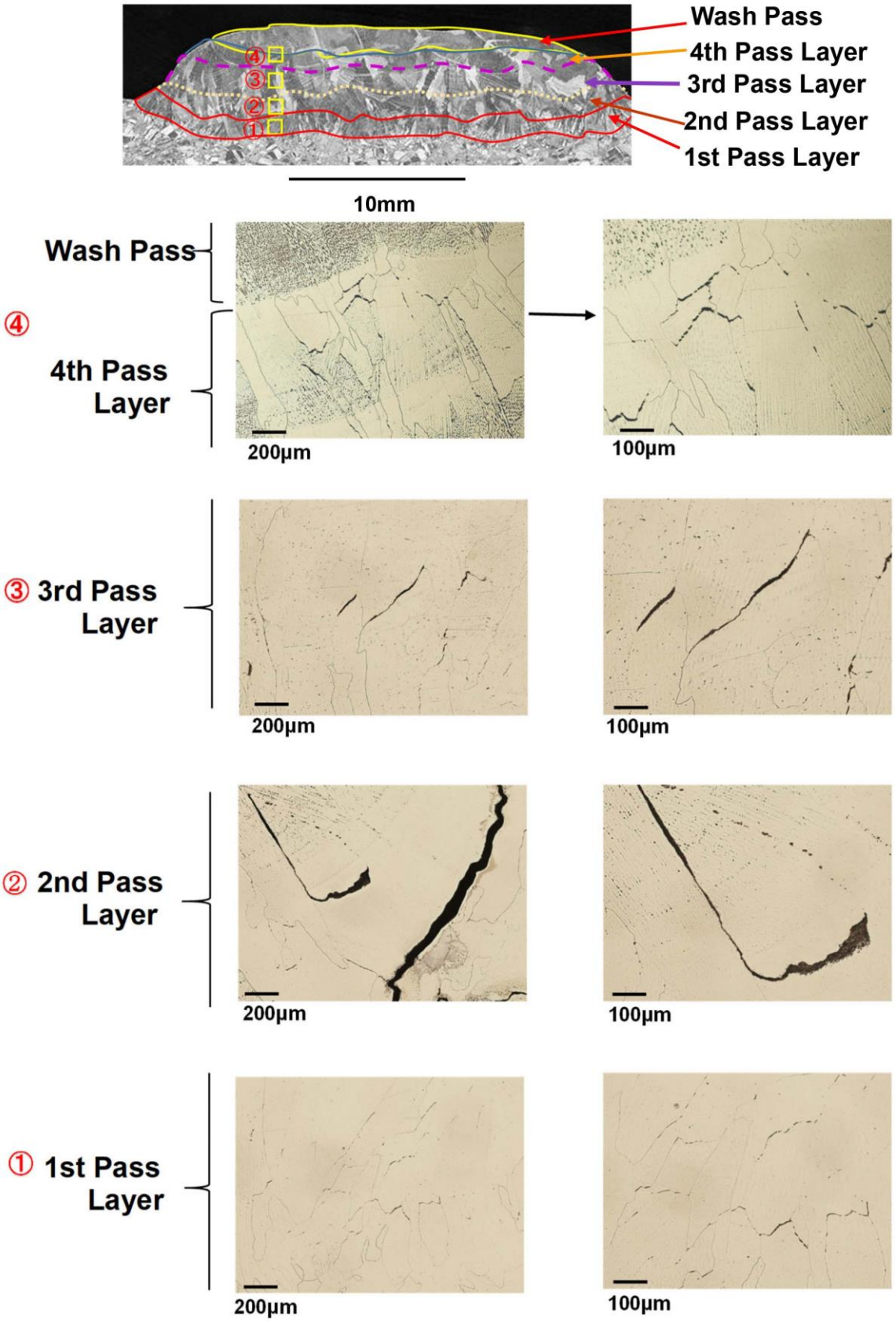

Fig.13 Comparison of DDC types in each layer of beads observed on the cross-section of FPFLB test specimen of Heat VT material.

481 **B**. ***Effect of Alloying on Weld Cracking Susceptibility***

482 The materials such as laboratory melted Heat VT, WT, No.9, No.10 and 09R/TD9, which contain
483 extremely low levels of impurity elements, showed high resistance to cracking by the Longi-
484 Varestraint testing. It is well known that the presence of eutectic forming impurity elements, such as
485 Si, S, Al, etc., tends to cause solidification cracking and liquation cracking in welding[52]. Therefore,
486 the Longi-Varestraint test evaluates better the solidification cracking and/or liquation cracking
487 susceptibility, but it should not be considered as an appropriate test method for assessing the DDC
488 susceptibility.

489 The on-heating on-cooling hot ductility test showed in this study that the on-cooling test is more
490 sensitive to hot ductility loss than the on-heating test. The hot ductility loss by the on-cooling test for
491 the laboratory melted Heat 09R/TD9, which has an extremely low impurity content, was smaller than
492 that for the commercial Alloy 52. This result was very similar to that of the Longi-Varestraint test, and
493 therefore it can be considered that the on-heating on-cooling hot ductility test is also not an appropriate
494 test method for assessing the DDC susceptibility.

495 On the other hand, the applied strain for cracking in the ductility-dip temperature range for Alloy
496 52 in the STF test was higher than that for Heat 09R/TD9, which has an extremely low impurity
497 content. Thus, the effect of impurity elements on the cracking susceptibility by the STF test was
498 opposite to that of the Longi-Varestraint and on-cooling hot ductility tests.

499

500 **C**. ***Possible Mechanism of DDC and a New Evaluation Test Method for DDC***

501 **C.1** *Possible mechanism of DDC*

502 According to the Introduction section, the mechanism of DDC was previously explained by
503 Matsuda et al., that S, O, N and Al contents accelerate DDC, P content slightly accelerates it, and Si
504 and Mn contents suppress it[27]. Nakao et al. reported that DDC is caused by the grain boundary
505 segregation of S[37]. In response to these findings, Collins and Lippold et al. reported that the DDC is
506 caused by an elevated temperature grain boundary sliding mechanism and such sliding can be opposed

507 macroscopically by the formation of tortuous grain boundaries via a grain boundary pinning
508 mechanism[38-42].

509 However, these observations can not fully explain the fact that DDC appears more likely in multi-
510 layer weld metals. Therefore, McCracken reported that the DDC may be caused by a strain ratchetting
511 mechanism[43,44].

512 The authors agree with this hypothesis, and conducted FPFLB tests to reproduce DDC using multi-
513 layer weld metal for comparing the DDC susceptibility of various high-Cr Ni-base alloys. Moreover,
514 from the mechanics of materials point of view[45-47], a thermal strain ratchetting TPLTC DDC test using
515 all-deposited weld metal specimens was developed and conducted. As shown in Fig. 12, the DDC
516 susceptibility of various high-Cr Ni-base alloys by the FPFLB test and the TPLTC test is in an excellent
517 agreement convincing that the DDC mechanism is based on thermal strain ratchetting. Furthermore, it
518 was confirmed that the TPLTC test method easily reveals the DDC susceptibility.
519

520 **C2**. *A New Evaluation Test Method for DDC*

521 In this study, based on the assumption that DDC is caused by a thermal strain ratchetting
522 mechanism, the axial tensile preloaded thermal cycling (TPLTC) test as a new DDC test method that
523 generates the thermal strain ratchetting in the specimen simulating multi-layer welding was developed
524 and performed from the mechanics of materials point of view.

525 The thermal strain ratchetting is a phenomenon in which permanent deformation gradually grows
526 in the direction in which steady stress is acting, when repeated plastic deformation caused by thermal
527 stress is applied to a member to which steady mechanical stress is acting.[45-47] So, the authors expected
528 that if the thermal strain ratchetting mechanism is the true DDC mechanism, the DDC can be
529 reproduced for the all-deposited weld metal specimens by the thermal strain ratchetting test. The
530 thermal cycling test for the tensile preloaded round-notched specimens made of the all-deposited weld
531 metal was performed by three repetitions for Heats 09/TD9, commercial Alloy 52, Sim. 52MSS and
532 B1. Typical test results for all the test materials are shown in Figs. 14 to 17.

Heat 09R/TD9 did not show a decrease in ductility in the medium to high temperature range by the on-cooling hot ductility test, but the TPLTC test specimen fractured at the time of only 11 thermal cycles, as shown in Fig. 14. Commercial Alloy 52 TPLTC test specimen fractured at the time of 23 thermal cycles, as shown in Fig. 15. Heat Sim.52MSS, which is a simulated laboratory melted heat of Alloy 52MSS, TPLTC test specimen fractured at the time of 30 thermal cycles, as shown in Fig. 16. Heat B1, which is a controlled Nb and C content laboratory melt, TPLTC test specimen fractured at the time of 40 thermal cycles, as shown in Fig. 17. Thus, the all-deposited weld metal Heat Sim.52MSS showed a good DDC resistance, but the all-deposited weld metal Heat B1 showed even better DDC resistance in the TPLTC test. Fig. 18 presents the comparison of the various test results between the Longi-Varestraint, on-cooling hot ductility, FPFLB and TPLTC tests. The results of the TPLTC test are very similar to the results of the FPFLB test, but the results of the Longi-Varestraint test and the on-cooling hot ductility test are quite different from the results of the TPLTC test and the FPFLB test. Based on these test results, it is considered that the TPLTC test is capable to evaluate the DDC susceptibility of the high-Cr Ni-base Alloy 52 variants easily and quantitatively.

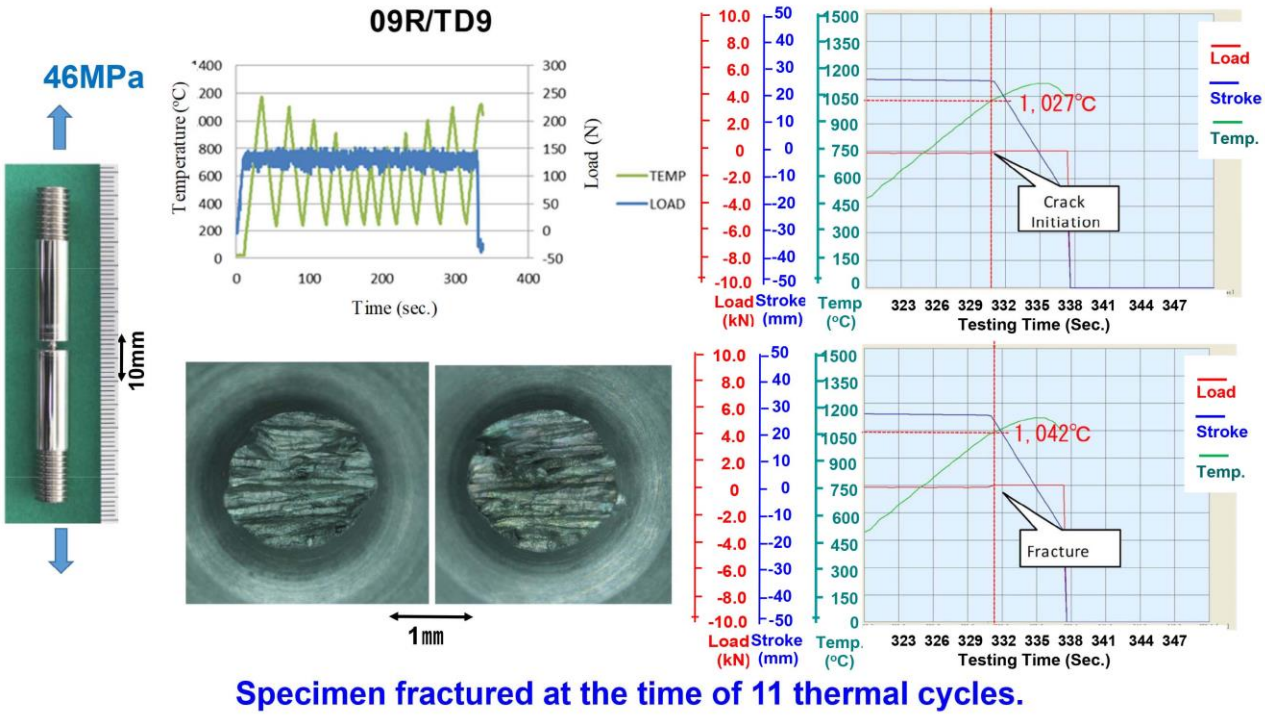

Fig. 14 TPLTC test results for laboratory melted Heat 09R/TD9.

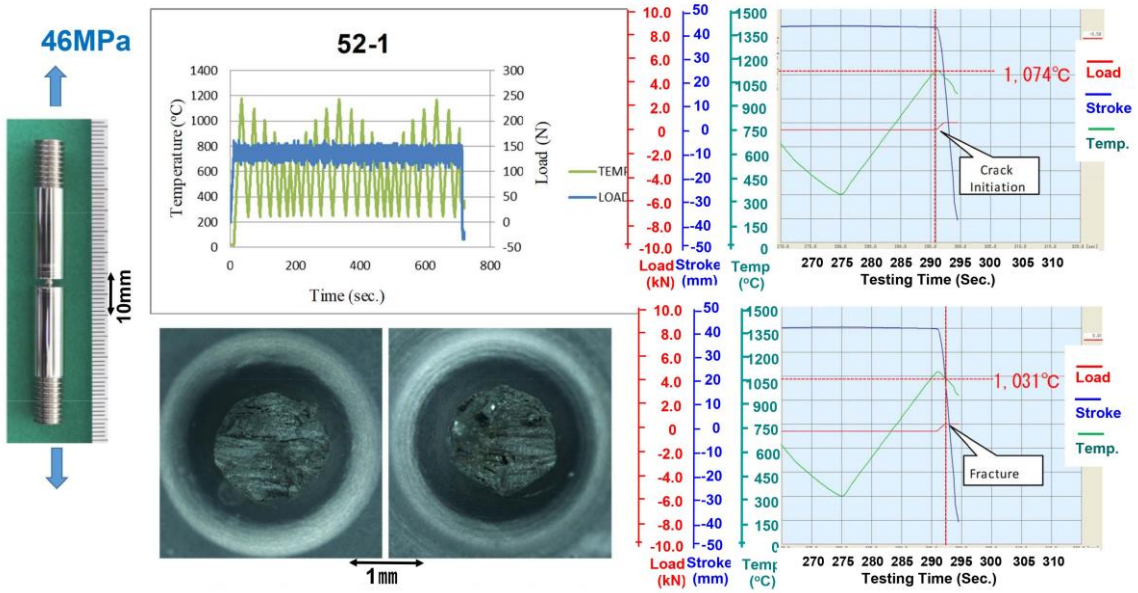

549 Fig. 15 TPLTC test results for commercial Alloy 52.

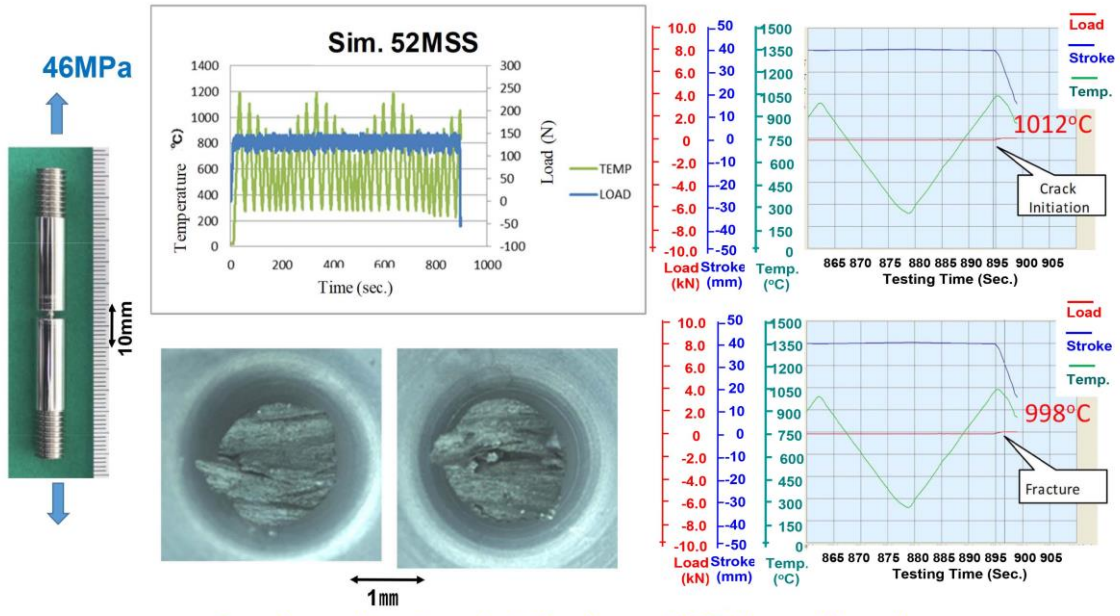

560 Fig. 16 TPLTC test results for laboratory melted Heat Sim.52MSS.

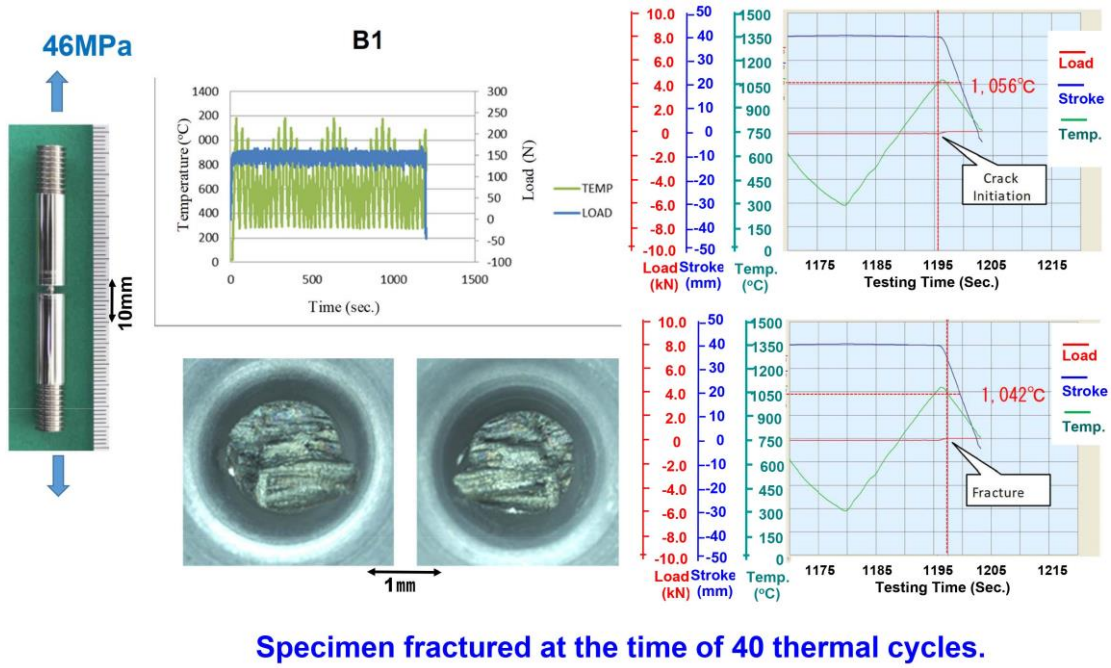

Fig. 17 TPLTC test results for laboratory melted Heat B1.

Alloy	Chemical Composition	Weld Cracking Test				
		Longi-Varestraint	On-cooling Hot Ductility	STF	FPFLB	TPLTC
Alloy52	0.027C-29Cr-9Fe-0.7Al-0.01Nb-0.5Ti	×	×	○	○	○
09R/ TD9	0.005C-30Cr-2.6Fe-0.06Al-0.002Nb-0.003Ti	◎	◎	×	△	× or △
WT	0.020C-30Cr-8.9Fe-0.086Al-0.069Nb-0.35Ti	◎	-	-	×	-
VT	0.016C-30Cr-8.9Fe-0.046Al-0.10Nb-0.25Ti	○	-	-	×	-
B2	0.023C-30Cr-8.1Fe-0.19Al-1.97Nb-0.30Ti	○	-	-	◎	-
Sim. 52MSS	0.020C-30Cr-3.0Fe-4.0Mo-0.19Al-2.47Nb-0.30Ti	△	-	-	◎	◎
B1	0.030C-30Cr-6.9Fe-0.19Al-2.47Nb-0.30Ti	△	-	-	◎	◉

Weld Cracking Susceptibility: ◉ < ◎ < ○ < △ < ×

Fig. 18 Comparison for the weld cracking susceptibility between Longi-Varestraint, on-cooling hot ductility, STF, FPFLB and TPLTC tests.

D, *Possible New DDC Resistant Welding Material*

In the Longi-Varestraint test, Heats No. 1 to No. 8 containing Al, Nb, Ti and Si, which tend to form eutectic phases, showed large values of both the number of cracks and the total crack length, as shown in Figs. 7 a) and 7 b). Most of the cracks were found in the weld bead, and many cracks are long. So, it is considered that the cracks are caused by solidification cracking. In fact, the 09R material, which has a low C, Al, Nb, Ti and Si content, and the commercial Alloy 52, which contains certain amount of C, were subjected to both the Longi-Varestraint test and the FPFLB test. The Heat 09R/TD9 showed excellent cracking resistance in the Longi-Varestraint test, as shown in Figs. 7 a) and 7 b), but was highly susceptible to cracking in the FPFLB test, as shown in Figs. 11 and 12. Commercial Alloy 52 was not so susceptible to cracking in the FPFLB test. Thus, when the contents of Al, Nb, Ti and Si are reduced, the solidification cracking resistance is improved, but the DDC resistance is presumed to be improved by certain amount of C and the precipitation of carbides.

In this study, the TPLTC test was performed by changing the amounts of Ti, Nb, and C, which tend to form carbides. As the result, the B1 material containing certain amount of Nb and C shows the best DDC resistance, as can be seen in Figs. 14 to 17. Sim.52MSS has the same amount of Nb, but the content of C is lower than that of material B1, resulting in a higher cracking susceptibility in the TPLTC test.

These tendencies are clearly confirmed in Fig. 18. The material B1 showed excellent resistance to DDC by FPFLB and TPLTC tests. Based on these data, the authors suggest that a Nb and C containing 30%Cr Ni-base Fe alloy without Mo is an advantageous new DDC resistant weld metal. The authors also consider that the Mo or W alloying may not have a beneficial effect on the DDC resistance.

IV. CONCLUSIONS

The weld cracking susceptibility by the Longi-Varestraint test, on-cooling hot ductility test, STF test, FPFLB test and TPLTC test for the laboratory melted alloys (totally 17 heats) of the 30%Cr Ni-base Fe alloy and commercial Alloy 52 were compared. Based on the test results, in the Longi-

Varestraint test the solidification cracking susceptibility increases in the alloys containing a large amount of the eutectic elements such as Si, Al, Nb and Ti, and the similar tendency was also detected by on-cooling hot ductility test. The STF test, FPFLB test and TPLTC test are capable to evaluate the DDC susceptibility of the high-Cr Ni-base Alloy 52 variants, and especially the TPLTC test is capable to evaluate the DDC susceptibility easily and quantitatively.

In order to evaluate the effect of thermal cycling on the DDC susceptibility, FPFLB test and the novel TPLTC test were conducted for the laboratory melted Heats 09/TD9, B1 and commercial Alloy 52. The results of FPFLB and TPLTC tests were quite different from those of the Longi-Varestraint and on-cooling hot ductility tests and the TPLTC test was capable to evaluate the DDC susceptibility of the high-Cr Ni-base Alloy 52 variants quantitatively. Based on the results of the TPLTC tests for laboratory melted heats and commercial Alloy 52, certain amount of Nb and C (for example 2.5 Nb and 0.03 C) containing Ni-based 30%Cr-Fe alloy without Mo is suggested advantageous as a new DDC resistant high-Cr Ni-base Alloy 52 variant.

V. ACKNOWLEDGEMENTS

This study was performed as a part of the collaboration research program between Tohoku University and Aalto University financially supported by Mitsubishi Heavy Industries, Ltd., Japan and Structural Integrity of Ni-base Alloy Welds-project (SINI) of Tekes, Finland. This study was accomplished by challenging welding and cracking tests. The authors thank Dr. Yuichi Miyahara, Mr. Mikko Peltonen, Mr. Anssi Brederholm and Dr. Teemu Sarikka for their valuable contributions in experiments and discussions.

On behalf of all authors, the corresponding author states that there is no conflict of interest.

REFERENCES

1. DuPont JN, Robino CV, Marder AR (1998) Solidification and Weldability of Nb-Bearing Superalloys. Welding J 77(10), pp.417s - 431s.
2. Bengough GD (1912) A Study of the Properties of Alloys at High Temperatures. The Journal of the Institute of Metals VII, pp.123 – 174.
3. Hudson OF (1912), Comments, The Journal of the Institute of Metals VII, pp.182 – 183.
4. Newell HD (1933) The Performance of 18-8 at High Temperatures. The Book of Stainless Steel, The American Society for Metals:364.
5. Kalish HS and Dunkerley FJ (1949) The Low-Temperature Properties of Tin and Tin-Lead Alloys. Trans. American Institute of Mining, Metallurgical Engineers 180, pp.637 – 656.
6. Carreker RP and Guard RW (1956) Tensile Deformation of Molybdenum as a Function of Temperature and Strain Rate. American Institute of Mining, Metallurgical and Petroleum Engineers Transactions 206, pp.178 – 184.
7. Pugh JW (1957) Temperature Dependence of the Tensile Properties of Vanadium. Trans. American Institute of Mining, Metallurgical and Petroleum Engineers Transactions 209, pp.1243 – 1244.
8. Rhines FN and Wray PJ (1961) Investigation of the Intermediate Temperature Ductility Minimum in Metals. Trans. American Society of Metals 54, pp.117 – 128.
9. Savage WF, Lundin CD (1965) The Varestraint test. Welding J 44(10), pp.433-s - 442-s.
10. Savage WF, Lundin CD (1966) Application of the Varestraint Technique to the Study of Weldability. Welding J 44(12), pp.497-s - 503-s.
11. Senda T, Matsuda F, Takano G Watanabe K, Matsusaka T (1971) Fundamental Investigation on Solidification Crack Susceptibility for Weld Metals with Trans-Varestraint Test. Trans JWS 2(2), pp.141 – 162.
12. Lippold J C (1983) An Investigaton of Heat-Affected Zone Hot Cracking in Alloy 800. Welding J 62(1), pp.1-s - 11-s.

13. Lippold JC (1992) Heat-Affected Zone Liquation Cracking in Austenitic and Duplex Stainless Steels. Welding J 71(1), pp.1-s - 14-s.
14. Lin W, Lippold JC, Baeslack Ⅲ WA (1993) An Evaluation of Heat-Affected Zone Liquation Cracking Susceptibility, Part I: Development of a Method for Quantification. Welding J 72(4), pp.135-s - 153-s.
15. Savage WF, Dickinson DW (1972) Electron Microanalysis of Backfilled Hot Cracks in Inconel 600. Welding J 51(11), pp.555-s - 562-s.
16. Savage WF, Nippes EF, Goodwin GM (1977) Effect of Minor Elements on Hot-Cracking Tendencies of Inconel 600. Welding J 56(4), pp.245-s – 253-s.
17. Ogawa T, Tsunetomi E (1982) Hot Cracking Susceptibility of Austenitic Stainless Steels. Welding J 61(3), pp.82-s - 93-s.
18. Nelson DE, Baeslack Ⅲ WA, Lippold J C (1987) An Investigation of Weld Hot Cracking in Duplex Stainless Steels. Welding J 66(8), pp.241-s - 250-s.
19. Baeslack Ⅲ WA, Lata WP, West SL, (1988) A Study of Heat-Affected Zone and Weld Metal Liquation Cracking in Alloy 903. Welding J 67(4), pp.77-s - 87-s.
20. Shankar V, Gill TPS, Mannan SL, Sundaresan S (1998) Evaluation of Hot Cracking in Nitrogen-Bearing and Fully Austenitic Stainless Steel Weldments. Welding J 77(5), pp.193-s - 201-s.
21. Ramsey PW, Keidel RA, Kuhr JN (1960) Hot-Cracking Teat for CO_2-Shielded Metal-Arc Weld. Welding J 39(5), pp.219-s - 224-s.
22. Goodwin GM (1987) Development of a New Hot-Cracking Test-The Sigmajig. Welding J 66(2), pp.33-s - 38-s.
23. Zacharia T, (1994) Dynamic Stresses in Weld Metal Hot Cracking. Welding J 73(7), pp.164-s - 172-s
24. Nelson TW, Lippold JC, Lin W, Baeslack Ⅲ WA (1997) Evaluation of the Circular Patch Test for Assessing Weld Solidification Cracking, Part Ⅰ-Development of a Test Method. Welding J 76(3), pp.110-s - 119-s.

671 25. Brown RS, Koch JB (1978) Development of Solidification Crack Resistant Weld Filler Metal for
672 a Stabilized Fully Austenitic Alloy. Welding J 57(2), pp.38-s - 42-s.
673 26. Warren FS, Boris MK (1966) An Investigation of Hot Cracking in Hastelloy X. Welding J 45(1),
674 pp.13-s - 25-s.
675 27. Matsuda F, Nakagawa H, Minehisa S, Sakabata N, Ejima A, Nohara K (1984) Weldability of Fe-
676 36%Ni Alloy (Report II) – Effect of Chemical Composition on Reheated Hot Cracking in Weld
677 Metal. Trans. of JWRI 13(2), pp.69 – 75.
678 28. Lundin CD, Delong WT, Spond DF (~~1975~~1976) The Fissure Bend Test. Welding J 55(6) Res.
679 Suppl., pp. 145-s - 151-s.
680 29. Lundin CD, Chou PD (1989) Hot Cracking Susceptibility of Austenitic Stainless Steel Weld Metals,
681 Welding Research Council Bulletin, 289.
682 30. Nissley NE, Collins MG, Guaytima G, Lippold J C Development of the Strain-to-Fracture Test for
683 Evaluating Ductility-Dip Cracking in Austenitic Stainless Steels and Ni-base Alloys. Welding in
684 the World 46(7-8), pp.32 – 40.
685 31. Nissley NE, Lippold JC (2003) Development of the Strain-to-Fracture Test. Welding J 82(12),
686 pp.355-s - 364-s.
687 32. Nissley NE, Lippold J C, (2003) Ductility-Dip Cracking Susceptibility of Austenitic Alloys. Proc.
688 6th International Trends in Welding Research, ASM International, pp.64 – 69.
689 33. Lippold JC (2005) Recent Developments in Weldability Testing for Advanced Materials, 2005.
690 Proc. International Conference on Joining of Advanced & Specialty Materials ASM International.
691 34. Nissley NE, Lippold JC (2008) Ductility-Dip Cracking Susceptibility of Nickel-Based Weld
692 Metals: Part 1, Strain-to-Fracture Testing. Welding J 87(10), pp.257-s - 264-s.
693 35. Noecker II FF, DuPont JN (2009) Metallurgical Investigation into Ductility Dip Cracking in Ni-
694 Based Alloys: Part I. Welding J 88(1), pp.7-s - 19-s.
695 36. Noecker II FF, DuPont JN, Metallurgical Investigation into Ductility Dip Cracking in Ni-Based
696 Alloys: Part II. Welding J. 88(3), pp.62-s - 77-s.

37. Nakao Y, Shinozaki K, Ogawa T, Sakurai H (1993) Effect of Cr and S on Ductility-dip Cracking Susceptibilities in Reheated Weld Metals of Ni-Cr-Fe Ternary Alloys – Study on Microcracks in Multipass Weld Metals of Ni-base Alloys (Part 2). Trans of the Japan Welding Society 24(2), pp.101 – 106.

38. Collins MG, Lippold JC (2003) An Investigation of Ductility Dip Cracking in Nickel-Based Filler Materials – Part I. Welding J. 82(10), pp.288-s - 295-s.

39. Collins MG, Ramirez AJ, Lippold JC (2004) An Investigation of Ductility Dip Cracking in Nickel-Based Filler Materials – Part III. Welding J. 83(2), pp.39-s - 49-s.

40. Ramirez AJ, Lippold JC (2004) High temperature behavior of Ni-base weld metal, Part I. Ductility and microstructural characterization. Materials Science and Engineering A 380, pp.259-271.

41. Ramirez AJ, Lippold JC (2004) High temperature behavior of Ni-base weld metal, Part II – Insight into the mechanism for ductility dip cracking. Materials Science and Engineering A 380, pp.245-258.

42. Nissley NE, Lippold JC (2009) Ductility-Dip Cracking Susceptibility of Nickel-Based Weld Metals: Part 2 - Microstructural Characterization. Welding J. 88(6), pp.131-s - 140-s.

43. McCracken SL, Tatman JK (2016) Comparison of Ductility-Dip Cracking to Computer Modeling with Sysweld^{TM} in a Narrow Groove Multi-Pass Weld. Proc. of the 2016 ASME Pressure Vessels & Piping Division Conference PVP-2016, July 17-21, Vancouver, BC, Canada, PVP 2016-63846.

44. McCracken SL, Tatman JK (2016) Prediction of Ductility-Dip Cracking in Narrow Groove Welds Using Computer Simulation of Strain Accumulation. Cracking Phenomena in Welds IV, Springer, pp.119 – 141.

45. Roche R.L, Moulin D, Lebey J (1982) Practical Analysis of Ratchetting. Nuclear Engineering and Design, 2 July, pp.51-66.

46. Manson SS (1966) Thermal Stress and Low-Cycle Fatigue. 184 McGraw-Hill.

47. Nakane K, Ohno N, Tsuda M, Yagi Y, Nakagawa I, Atsumi T (2008) Thermal Ratcheting of Solder-Bonded Elastic and Elastoplastic Layers. International Journal of Plasticity 24(10),

723 pp.1819 – 1836.
724 48. Luther SJ, Alexandrov BT (2021) Recreating Ductility-Dip Cracking via Gleeble–Based Welding
725 Simulation. Welding J 100(1), pp.27-s - 39-s.
726 49. Luther SJ, Alexandrov BT, McCracken SL, Tatman JK (2022) Correlation of Imposed Mechanical
727 Energy with Ductility-Dip Cracking in a Highly Restrained Weld of Alloy 52. J of Manufacturing
728 Process 79, pp.767 – 788.
729 50. Kiser S, Zhang R, Caruso M (2012) New Technical Data and Commercial Applications for 30%
730 Cr Nickel Alloy Nuclear Welding Products 52MSS and 152MSS. Proc. Welding and Repair
731 Technology for Power Plants, Tenth International EPRI Conference, June 26-29, 2012.
732 51. Lippold JC, Nissley NE (2006) Further Investigations of Ductility-Dip Cracking in High
733 Chromium, Ni-base Filler Metals. IIW-IIC-326-06 Quebec City, Canada.
734 52. Yonezawa T (2020) Nickel-Based Alloys, Comprehensive Nuclear Materials (Second Edition),
735 Vol.7, pp. 233-266.
736